ISSN NO. 2320-5407

Journal homepage:http://www.journalijar.com

INTERNATIONAL JOURNAL OF ADVANCED RESEARCH

RESEARCH ARTICLE

Removal of calmagite dye from aqueous media using nanoparticles of mango seed kernel–impregnated Fe (III)

Salwa A. Ahmed*, Ahmed A. Abdel Gaber & Asmaa M. Abdel Rahim
Chemistry department, Faculty of science, Minia University, Minia, Egypt

Manuscript Info *Abstract*

Manuscript History:

Received: 14 December 2014
Final Accepted: 25 January 2015
Published Online: February 2015

Key words:

Adsorption,
Calmagite,nanoparticles of mango seed kernel, Fe(III), Removal

Corresponding Author

Salwa A. Ahmed

This manuscript combines both the advantages of the high surface area of nanoparticles and the strong high affinity of Fe(III) for reacting with calmagite dye. So, a novel, simple, benign and eco-friendly nanoparticles adsorbent of mango seed kernel–impregnated Fe(III) (NPs-MSK-Fe) was developed. It was characterized by Fourier transform infrared spectroscopy, transition and scanning electron microscopy and X-ray diffraction. The adsorption characteristics were examined using effective parameters including the effect of pH, equilibrium time, adsorbent amount and dye concentration. The adsorption percent of calmagite using NPs-MSK-Fe was found to be 98.86 % at pH = 2.0. Regeneration of the NPs-MSK-Fe was achieved in acidic ethanol solutions to recover both the adsorbent and the desorbed dye. The regenerated adsorbent can be reused for calmagite removal and the adsorption percent is still 98.86 % after reused for three times. Finally, the new adsorbent was used successfully for the removal of calmagite dye from different environmental water samples.

INTRODUCTION

Calmagite dye is one of synthetic azo-dyes which widely used in textile industries, cosmetic, paper, drug and food processing industries in largest quantities (Pinheiro et al., 2004). Its effluent is hard to treat, high in volume and made of harmful organic and inorganic chemicals that exhibit toxic and carcinogenic effects toward biological systems (Kroschwitz and Howe-Grant, 1993). Therefore, the presence of this synthetic dye in water causes considerable environmental pollution. Different processing technologies including solid phase extraction (SPE) being used for adsorption and removal of dye contribute in water pollution. It offers high efficiency, cost effectiveness and easy handling among the majority of physiochemical treatment methods (Luo et al., 2011). Recently, cheaper and effective adsorbents can be formed from numerous natural materials or certain waste materials from industrial and agricultural activities. The agricultural waste materials are economic and environment friendly due to their chemical composition, their availability, renewable nature and low cost which viable option for water and wastewater treatment. The basic components of these waste materials include hemicellulose, lignin, lipids, proteins, simple sugars, water, hydrocarbons, starch, and contain variety of functional groups (Bhatnagar and Sillanpää, 2010). These agricultural waste materials have been used in their natural form or after some physical or chemical modification with organic functional groups to increase their efficiency for removal of pollutants (Yu et al. 2009; Singh and Srivastava, 1999). Various numbers of these wastes have been developed as adsorbents for removal of dyes, like sugar cane bagasse ash (Kanawade et al., 2010), sawdust (Hamdaoui, 2006), fly ash (Bello et al., 2013), tea waste (Madrakianet. Al, 2012) and apricot stones (Demirbas et al., 2008). Among these agricultural waste materials, mango seed kernel was of little use as adsorbent for removal of pollutants from water (Kumara andKumaranb, 2005;Elizalde-Gonzàlez and Hernàndez-Montoya, 2007). It is rich in functional groups that have a high metal binding capability. This kernel contains the most of the essential amino acids such as leucine and valine

(Diaz and Coto, 1983) and is a rich source of gallic acid (Soong and Barlow, 2006) that can be complexed with Fe(III) (Fazary et al., 2009). On the other hand, to increase the efficiency of adsorbent recent researches have turned to the use of nanoparticles due to their large specific surface area that can reveal a wide variety of interactions, depending on their nature, with target analytes. Furthermore, the nanometric dimension provides the material with a new physicochemical properties and small internal diffusion resistance (Dou et al., 2011) which can be very effective for adsorbing heavy metals and organic pollutants from waste water. To our knowledge, there is no study of using waste materials in nanoparticles size. So, the big challenge in our study is to obtain low cost adsorbent with high surface area through development to nanoparticles of mango seed kernel (NPs-MSK). For increasing the selectivity and loading capacity of adsorbent surface some chemicals such as metal ions have been used for modifications but with complicated procedures (Namasivayam and Sangeetha, 2006). For this reason, modification and impregnation techniques were used to increase surface adsorption and removal capacity of adsorbent (Adhoum and Monser, 2002; Soliman et al., 2013; Ghanizadeh et al., 2010).

So, the main objective of this paper is to develop a new and simple method for modification ofNPs-MSK surface through impregnated with Fe(III) which has the ability to bind with calmagite dye (Soylak et al., 2002). This new adsorbent was used successfully for the removal of calmagite dye from different environmental water samples.

2. Materials and methods

2.1. Chemicals

Fresh mangoes were obtained from a local market in Minia, Egypt. Doubly distilled water (DDW) was used throughout all experiments. Ferric chloride ($FeCl_3.6H_2O$), ethanol and calmagite dye were analytical grade from Merck, Germany. ACS reagent grade hydrochloric acid and sodium hydroxide were obtained from Aldrich. Samples of Nile River water (NRW), drinking tap-water (DTW) and ground water (GW) were collected from Minia. Also, sample of waste water (WW) was taken near the drainage of the sugar plant in Minia, Egypt.

2.2. Adsorbent preparation

2.2.1. Preparation of nanoparticles mango seed kernel

The seeds (four samples) were removed manually using stainless steel knives and were opened to get kernels. The kernels were washed with DDW and air dried. The dried material was ground in a mill and sieved to obtain a powdery form and remove the large particles. The powdered form was also ground and sieved another time.The final powdered material was washed with DDW and dried well in an oven at 60 °C for 1h. Then, it was kept in a closed dark glass bottles and stored until utilization. The particle size of the powdered materials ranged from 11.0−17.0 nm.

2.2.2. Modification of nanoparticles mango seed kernel

(a) Adsorption studies of nanoparticles mango seed kernel with Fe(III)

The prepared nanoparticles of mango seed kernel (NPs-MSK) was used firstly as adsorbent to obtain the optimum conditions for uptake of Fe(III). The metal uptake capacity and adsorption percent of such NPs-MSK adsorbent towards Fe(III) were determined in triplicate under static conditions by the batch equilibrium technique. 20.0 mg of the adsorbent was transferred to a 100.0 mL volumetric flask containing 0.5 mL of Fe(III) solution (the actual concentration of the prepared Fe(III) solution was determined using EDTA titration). Appropriate volumes of 1.0 M HCl or 1.0 M NaOH for adjustment the pH values (2.0 – 4.0). The resultant mixture was completed to 50.0 mL with DDW. This mixture was mechanically shaken for 30 mins at room temperature to attain equilibrium. Then the solid phase was separated by filtration, washed with DDW and the unretained metal ion in the filtrate was determined by complexometric EDTA titration (Ahmed, 2011). The effect of shaking time, amount of adsorbent and metal ion concentration were tested and evaluated by the same previous batch method. The optimum conditions were found to be: 20.0 mg of the adsorbent was introduced to 50.0 mL containing Fe(III) (0.05 mmol) solution and shaking for 15 min at pH 3.5. These conditions led to 100.0 % ± 0.1 extraction and 139.63 mg/g metal capacity of Fe(III) on NPs-MSK adsorbent, Table 1.

(b) Preparation of the nanoparticles mango seed kernel–impregnated Fe(III)

500.0 mg of NPs-MSK was soaked for two days in 50.0 mL of 0.5 M $FeCl_3.6H_2O$ solution (its pH was adjusted to 3.5 by adding drops of 1.0 M NaOH and 1.0 M HCl). Then this mixture was filtrated and washed with DDW in order to remove the residues of $FeCl_3$ as the filtrate being colorless. The modified phase was left to dry in an oven at 60 °C for 1h. A confirmation that the modification process has successfully achieved it was found that the mango seed kernel color changed from white to black one, Fig. 1. The particle size of NPs-MSK-Fe adsorbent was ranged from 12.4 to 15.4 nm.

2.3. Adsorbent characterization

The surface functional groups of NPs-MSK and NPs-MSK-Fe were analyzed by Fourier transform infrared (FT-IR) spectroscopy (410 JASCO, Japan). The particle size and surface morphology of the adsorbents were characterized using transition electron microscopy (JEM100CX11 JEOL, Japan) and scanning electron microscopy (JSM-5400 LV JEOL, Japan). The crystal structureof the adsorbents was studied using X-ray diffractometer (JSX-60 PA JEOL, Japan).

2.4. Studies on point zero charge (pH_{zpc}) of adsorbent

In pH_{zpc} determination, 200 mg of each adsorbent (NPs-MSK and NPs-MSK-Fe) was added to 50.0 mL of 0.01 M NaCl and its pH was adjusted in the range of 2.0 – 12.0 by adding appropriate volumes of 1.0 M HCl or 1.0 M NaOH (Sharma et al., 2009). These flasks were kept for 48 h and final pH of the solution was measured by using Fisher Scientific Accumet pH-meter (Model 825, Germany). Graphs were then plotted for pH_{final} versus $pH_{initial}$.

2.5. Batch adsorption experiments

The adsorption experiments were carried out using batch method. Different parameters such as, effect of pH, dye concentration, adsorbent amount and contact time were studied. Definite weight of each adsorbent (NPs-MSK and NPs-MSK-Fe) was added to 50.0 mL of 1.0×10^{-4} M of calmagite dye. Different additions of 1.0 M NaOH or 1.0 M HCl solutions were used for justifying the pH values before adding the adsorbent. The solution was then shaken by Wrist Action mechanical shaker model 75 (manufactured by Burrell Corporation Pittsburgh. PA. U.S.A.) at different time intervals at room temperature to attain equilibrium. Subsequently, these solutions were filtered out by using filter paper. The filtrate after adsorption process was analyzed using UV/visible spectrometer (Perkin Elmer Lambda 35 UV/Visible spectrophotometer, England) by recording the absorbance changes at a wavelength of maximum absorbance (602 nm). The amount of dye adsorbed on the adsorbent surface was calculated from the concentrations difference in solutions before and after adsorption. All the adsorption experiments have been carried out in triplicate. The adsorption percentage of the dye adsorbed was calculated using the equation:

$$\%\, Removal\ (adsorption) = \frac{C_i - C_f}{C_i} \times 100$$

whereC_i is the initial concentration of dye and C_f is its final concentration.

2.6. Desorption and regeneration studies

Desorption measurements were conducted in order to explore the feasibility of recovering the analyte and the adsorbent. Six weights of 100.0 mg of saturated NPs-MSK-Fe adsorbent with calmagite dye were soaked in 25.0 mL of acidic ethanol solutions (ethanol: water, 1:1 v/v) at pH range from 1.0 to 6.0 in six measuring flasks. These mixtures were shaken for 1h, have been left overnight, and then were filtrated and washed thoroughly with DDW to a neutral pH. Each treated adsorbent was dried well to be reused for next experiment under the same previous conditions of batch method.

2.7. Removal of calmagite dye from environmental water samples

Different water samples drawn from Nile River water (NRW), drinking tap-water (DTW), waste water (WW) and ground water (GW) were collected and stored in clean polyethylene bottles. The water samples were filtered before the analysis to remove any insoluble substances. 50.0 mg of NPs-MSK-Fe was conditioned with 50.0 mL of each water sample spiked with 3.0 mL of 1×10^{-4}mol/L of calmagite dye after adjusting the pH of samples to the optimum pH value and shaking for 30 min. Each filtrate was taken and the concentration of dye was determined by UV/visible spectrometer using the previous procedure as described above.

3. Result and discussion

3.1. Characterization of adsorbent

3.1.1. FT-IR

The FT-IR spectra for nanoparticles of mango seed kernel (NPs-MSK) and nanoparticles of mango seed kernel–impregnated Fe(III) (NPs-MSK-Fe) were shown in Fig. 2. The NPs-MSK spectrum displays a number of absorption peaks, reflecting its complex nature. A strong and broad peak at 3385 cm^{-1} could be assigned to stretching υ(N–H) of amino groups or υ(O–H) stretching vibrations mode of hydroxyl functional groups. A change

in peak position to 3364 cm^{-1} in the spectrum of NPs-MSK-Fe indicates to the coordination of Fe(III) with amino and/or hydroxyl groups. The peak at 1645cm^{-1} was attributed to υ(C=O) group, which exist as functional groups of NPs-MSK and shifting of this peak to 1649 cm^{-1}, indicating to involvement of these groups in NPs-MSK-Fe phase (Salem et al., 2012). The shoulder peak in NPs-MSK at 1000 cm^{-1} due to υ(C–O) stretching vibrations (Elizalde-Gonzàlezb and Hernàndez-Montoya, 2007) was shifted to 1241 cm^{-1} in NPs-MSK-Fe. The small peaks observed in the region of 1455−1340 cm^{-1} were attributed to ether and carboxylate groups in NPs-MSK were splatted and shifted to 1461−1369 cm^{-1} in NPs-MSK-Fe adsorbent. The shifts in the absorption peaks generally emphasize that the modification process with Fe(III) taking place on the surface of the NPs-MSK. In addition, an obvious color change from white of NPs-MSK to black of NPs-MSK-Fe as illustrated in Fig. 1.

3.1.2. TEM and SEM

The particle size of NPs-MSK and NPsMSK-Fe was determined through TEM analysis. Fig. 3ashows the TEM of NPs-MSK adsorbent at 100 nm where the particles of the adsorbent have spherical shape with particle size range of 11.0−17.0 nm. As evident in Fig. 3b after the impregnation process of NPs-MSK, the Fe(III) occupied and gathered on the surface of NPs-MSK and tied in the form of clusters. The NPs-MSK-Fe adsorbent has an average diameter of about 12.4–15.4 nm.

The morphology of both the two adsorbents was examined by SEM analysis. SEM images for NPs-MSK and NPs-MSK-Fe were shown in Fig. 4. The NPs-MSK materials have porous surface which allowed binding of Fe(III) easily as shown in Fig. 4a. After binding with Fe(III) the adsorbent was completely covered with Fe(III), and all the Fe(III) were aggregated to form a spherical and cage-like structure (Panneerselvam et al., 2011), Fig. 4b.

3.1.3. X-ray

The X-ray diffraction spectra of the NPs-MSK and NPs-MSK-Fe adsorbents were shown in Fig. 5. NPs-MSK adsorbent showed A-type X-ray diffraction patterns (Sandhu and Lim, 2008) and showed strong reflections at 2θ ranges between 15º and 23º and an unresolved doublet at 17º and 18º. After impregnation of NPs-MSK with Fe(III), the bands of NPs-MSK was converted into sharp bands with higher intensities. Also, the peaks found at 37º, 53º and 83º were attributed to the presence of Fe(III) (Panayiot and Stjamesb, 2009). These changes of the structure of phases confirm the modification of the NPs-MSK surface.

3.2. Effect of pH on dye adsorption

The point of zero charge was found to be 4.0 for both NPs-MSK and NPs-MSK-Fe adsorbents using standard potentiometric method as illustrated in Fig. 6. Therefore, the surface charges of both two adsorbents were positively charged at pH < 4.0. It seems that at pH 1.0–3.0, most of $–NH_2$ and –OH groups are protonated, which are favorable for the adsorption of (acidic) calmagite dye (Reddy and Lee, 2013).According to the previous results, the batch experiments were performed at pH range 1.0 – 10.0 to find out the effect of pH on the adsorption of calmagite over NPs-MSK and NPs-MSK-Fe, Fig. 7(a, b). The two adsorbents showed maximum uptake values for calmagite dye at pH 2.0. However, it was found that the adsorption percent and capacity values of NPs-MSK-Fe adsorbent (98.86 % and 2125.7 µg g^{-1}) were higher than NPs-MSK adsorbent (67.84 % and 1458.7 µg g^{-1}). This behavior can be explained on the basis of the protonation of amino and hydroxyl groups at low pH as shown in the following equations: In the case of NPs-MSK adsorbent, the mechanism of the adsorption process of calmagite is likely to be the electrostatic interactions of the colored dye ions with the amino and hydroxyl groups of the NPs-MSK. In acidic solution (pH = 2.0), the calmagite dye was dissolved and converted to anionic dye ions having negatively charged sulfonic groups $D–SO_3^-$ (Reddy et al., 2007).

$$D–SO_3H \rightarrow D–SO_3^- + H^+$$

Also, in the presence of H^+, the amino and hydroxyl groups of the NPs-MSK$–NH_2$ and NPs-MSK–OH became protonated.

$$\text{NPs-MSK}–NH_2 + H^+ \leftrightarrow \text{NPs-MSK} –NH_3^+$$

$$\text{NPs-MSK}–OH + H^+ \leftrightarrow \text{NPs-MSK} –OH_2^+$$

Then, the adsorption process progressing due to the electrostatic attraction between the two oppositely charged ions as illustrated in Scheme 1.

On the other hand, for NPs-MSK-Fe adsorbent, the highest adsorption percent can be attributed to the complex formation and the electrostatic interactions. Firstly, binary complex was formed between amino and hydroxyl groups on NPs-MSK surface with Fe(III) due to impregnation process. After adsorption of calmagite dye, a ternary complex was formed between Fe(III) and hydroxyl groups in that dye (Fazary et al., 2009) . Also, the

amino groups on NPs-MSK-Fe adsorbent at low pH value became protonated as in the case of NPs-MSK, Scheme 2. This has been augmented by the higher values of adsorption percent of NPs-MSK-Fe than NPs-MSK which confirm that impregnation process improved the surface of NPs-MSK for uptake of calmagite dye. At high pH, the two adsorbents displayed a sharp decrease in the uptake values. Whereas in NPs-MSK adsorbent, the number of protonated $–NH_2$ and –OH groups will decrease at high pH and more OH^- ions will be available to compete with the anionic sulfonic group in calmagite dye (Reddy and Lee, 2013). In the case of NPs-MSK-Fe adsorbent, at pH> 4.0, the $Fe(OH)_3$ can be produced, therefore the adsorption percent for the acidic dye decreases (Sheibani et al., 2012).

3.3. Effect of adsorbent amount

The weights of the two adsorbents were varied from 10.0 to 200.0 mg keeping all the other experimental variables constant. The results in (Fig. 8) showed that, the adsorption percent of calmagite dye not affected by increasing the weight of NPs-MSK up to 200.0 mg with adsorption capacity of 1458.7 µg g^{-1}. But in the case of NPs-MSK-Fe, the adsorption percent increased with increasing the amounts of adsorbent up to 50.0 mg where adsorption capacity values ranged from up 820.7 to 2125.7 µg g^{-1}. It has been shown that the nano-sized adsorbents which have high surface areas gave satisfactory results through fewer amounts compared to the ordinary adsorbents (Dou et al., 2011). The impregnation process carried out increased the NPs-MSK-Fe capacity for adsorption of analyte. It was found that, more than 50.0 mg of NPs-MSK-Fe, the adsorption percent decreased. Such behavior was expected due to the saturation level attained during an adsorption process (Yagub et al., 2014).

3.4. Effect of equilibrium time

Equilibrium time is another important factor in the evaluation process of the new adsorbent. Adsorption percent values were determined using the batch method at different shaking times (5, 10, 15, 25, 30 and 60 min) to determine the time needed to attain equilibrium using the NPs-MSK and NPs-MSK-Fe adsorbents. The adsorption percent for calmagite dye at the optimum pH value was calculated at each time interval relative to highest uptake at 30 min for both the two adsorbents, (Fig. 9). It was found that, the adsorption percent of calmagite dye on 50.0 mg NPs-MSK-Fe equals 98.86 % but on 100.0 mg NPs-MSK equals 67.84 % at 30 min. This situation can be explained via the structure of dye as described above in Schemes 1 and 2 where calmagite dye has a greater opportunity for binding to the surface of the NPs-MSK-Fe adsorbent than NPs-MSK adsorbent.

3.5. Effect of dye concentration

The amount of adsorption for dye removal is highly dependent on the initial dye concentration. The effect of initial dye concentration depends on the immediate relation between the concentration of the dye and the available sites on an adsorbent surface (Sharma et al., 2010). At the optimum pH, 100.0 mg of NPs-MSK and 50.0 mg of NPs-MSK-Fe adsorbents were added to different concentration (2.0×10^{-6} – 20.0×10^{-6} mol/L) of calmagite dye, (Fig. 10). The increase in initial concentration enhances the interaction between adsorbent and dye. It has been found that the adsorption percent and metal capacity for both adsorbents were increased with concentrations $2.0 \times 10^{-6}$to 6.0×10^{-6} mol/L then decreased with the increase in dye concentration from 8.0×10^{-6} to 20.0×10^{-6} mol/L. This is due to the initial dye concentration provides the driving force to overcome the resistance to the mass transfer of dye between the aqueous and solid phase. Moreover, the adsorption percent and capacity of NPs-MSK-Fe (98.86 % and 2125.7 µg g^{-1}) were higher than those of NPs-MSK (67.84 % and 1458.7 µg g^{-1}) for 6.0×10^{-6} mol/L of dye. This described the rule of impregnation of NPs-MSK with Fe(III).

With this data, it was decided that NPs-MSK-Fe is the best adsorbent for extraction and removal of calmagite dye.

3.6. Desorption and regeneration studies

Desorption of sorbet from the adsorbent is very important and that which will provide the beneficial features including reusability of adsorbent, recovery of pollutants, reducing the process cost, reducing the generation of secondary wastes and identifying the adsorption mechanism (Reddy and Lee, 2013). In order to evaluate the possibility of regeneration and reuse of the NPs-MSK-Fe adsorbent, desorption experiments have been performed in acidic ethanol at pH range from 1.0 to 6.0. The results in (Fig. 11) show that the maximum desorption efficiency was 100.0 % ± 0.1 with acidic ethanol at pH = 6.0. The adsorption percent of NPs-MSK-Fe (98.86 %) for calmagite dye did not show any significant decrease but after three regenerations.

3.7. Removal of calmagite dye from environmental water samples

Dyes are an important class of pollutants which enter aquatic systems as a result of rapid industrialization (Gupta and Suhas, 2009). So, the new developed adsorbent NPs-MSK-Fe was applied for the removal of calmagite dye spiked environmental water samples by batch technique.As illustrated in Fig. 12, the recoveries for NRW,

DTW, WW and GW on NPs-MSK-Fe adsorbent were 99.0, 98.77, 100.0 and 99.56 %, respectively. These recovery values indicate the suitability and validity of using NPs-MSK-Fe adsorbent for removal of calmagite dye.

Table 1: Metal uptake capacities (mg/g) and adsorption percent of the NPs-MSK adsorbent at different pH values Recovery % values are based on N = 3

Adsorbent	pH value	Metal capacity (mg/g)	Adsorption percent
NPs-MSK	1.0	68.56	49.1 ± 0.1
	2.0	120.92	86.6 ± 0.05
	3.0	129.57	92.8 ± 0.1
	3.5	139.63	100.0 ± 0.1
	4.0	precipitation	precipitation

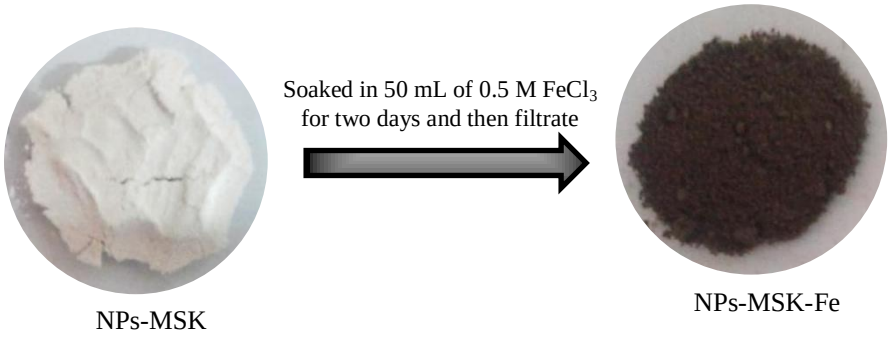

Figure 1: Impregnation of NPs-MSK adsorbent with Fe(III)

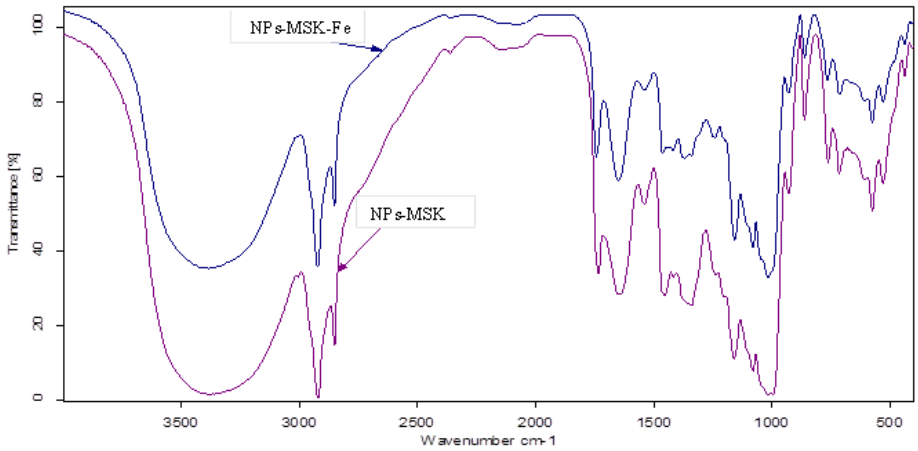

Figure 2: FT-IR spectra of NPs-MSK and NPs-MSK-Fe adsorbents

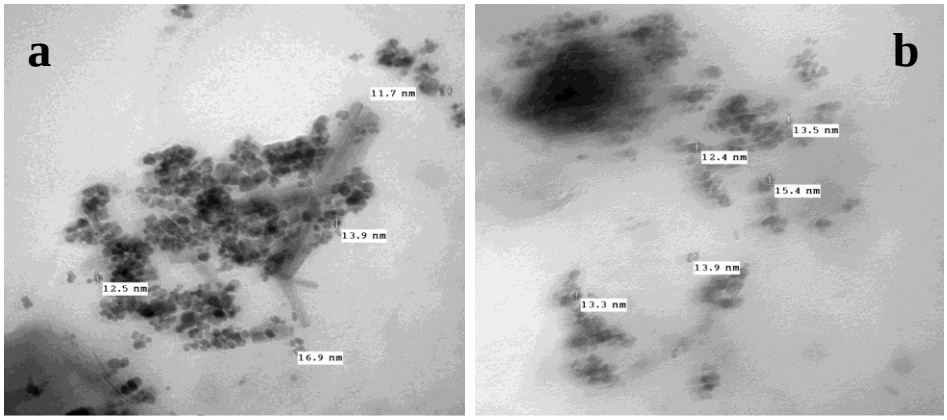

Figure 3: TEM image of (a) NPs-MSK and (b) NPs-MSK-Fe adsorbents

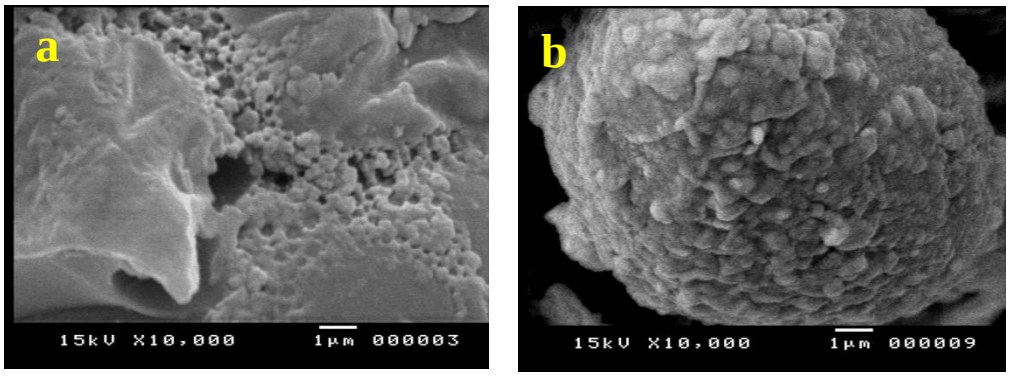

Figure 4: SEM image of (a) NPs-MSK and (b) NPs-MSK-Fe adsorbents

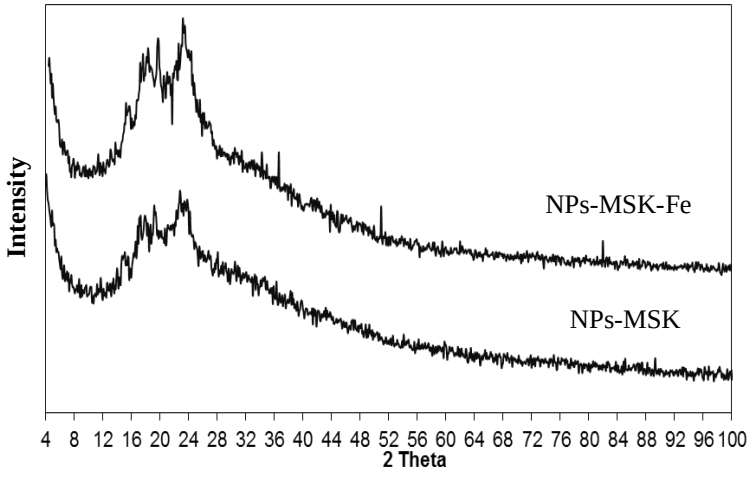

Figure 5: XRD patterns of NPs-MSK and NPs-MSK-Fe adsorbents

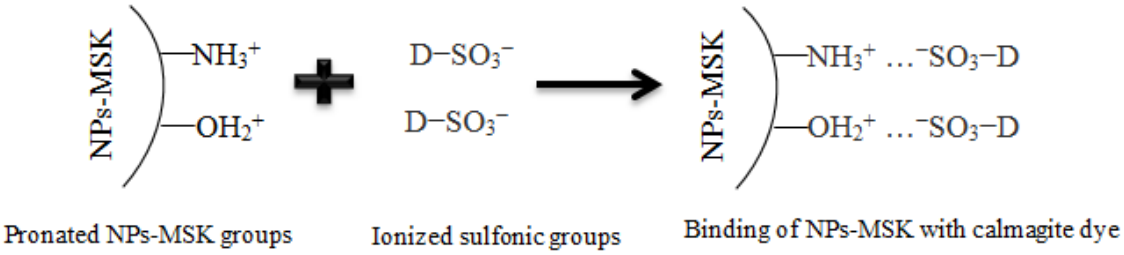

Scheme 1: Suggested mechanism of the ionic interaction between NPs-MSK and calmagite dye

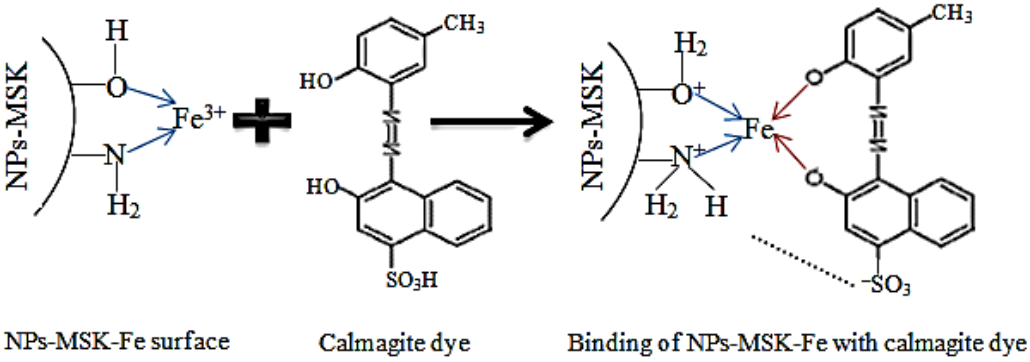

Scheme 2: Suggested mechanism of the ternary complex formation and ionic interaction between NPs-MSK-Fe and calmagite dye

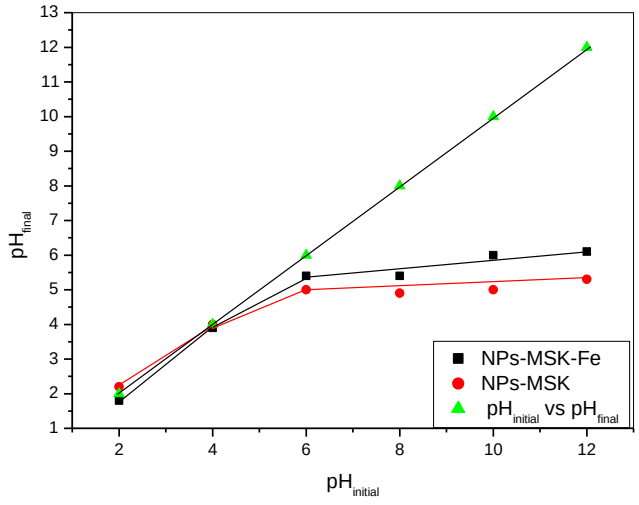

Figure 6: Plot for determination of point zero charge of NPs-MSK and NPs-MSK-Fe adsorbents

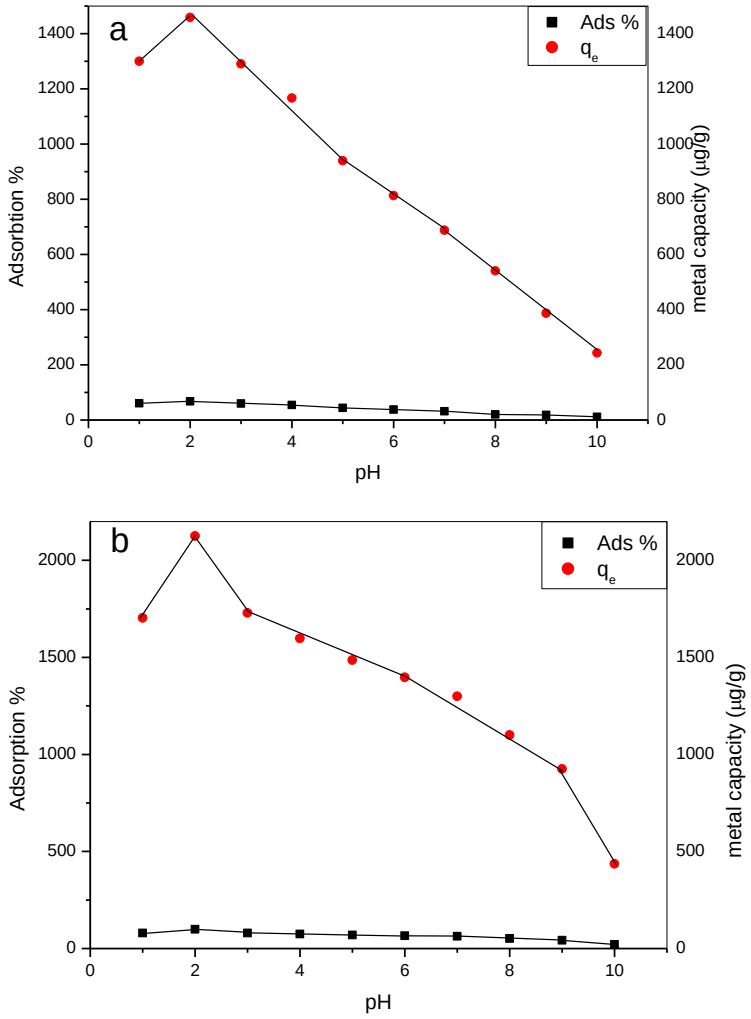

Figure 7: Effect of pH on adsorption percent and capacity values of (a) NPs-MSK and (b) NPs-MSK-Fe adsorbents

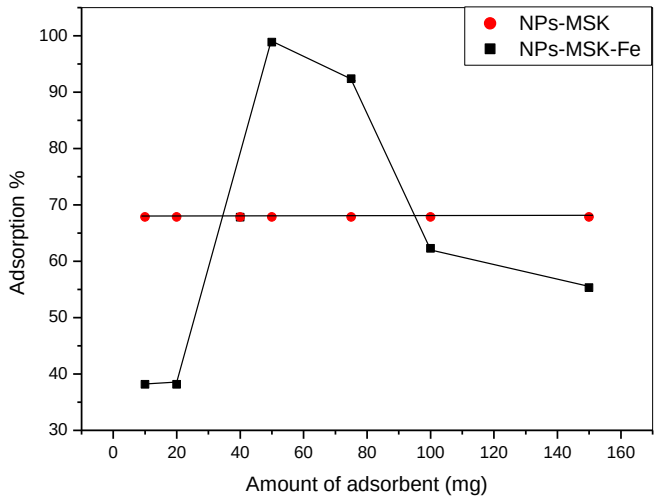

Figure 8: Effect of adsorbent amount on adsorption percent of NPs-MSK and NPs-MSK-Fe adsorbents

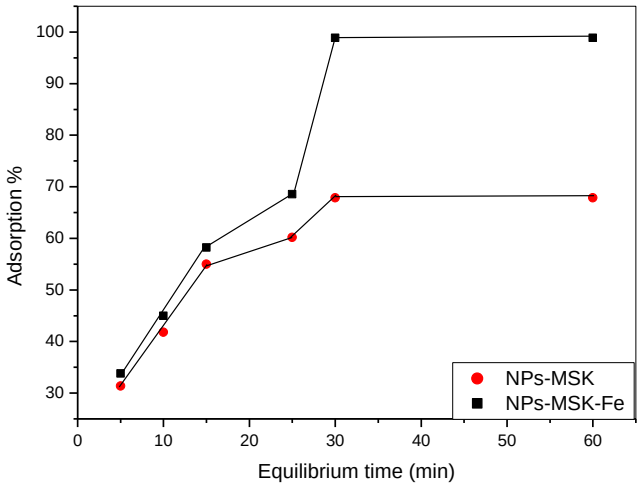

Figure 9: Effect of equilibrium time on adsorption percent of NPs-MSK and NPs-MSK-Fe adsorbents

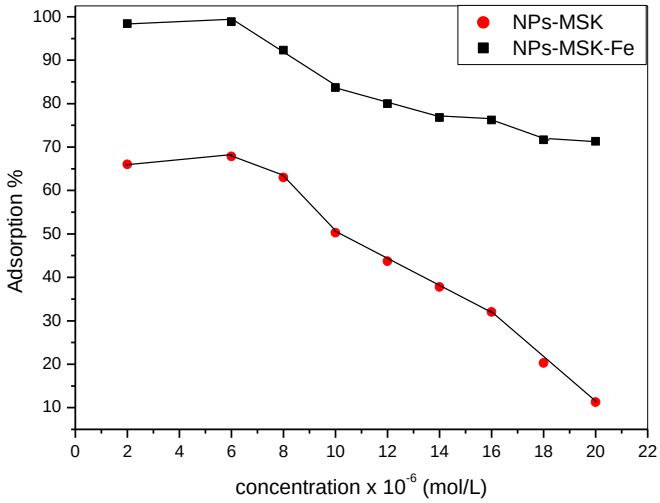

Figure 10: Effect of dye concentration on adsorption percent of NPs-MSK and NPs-MSK-Fe adsorbents

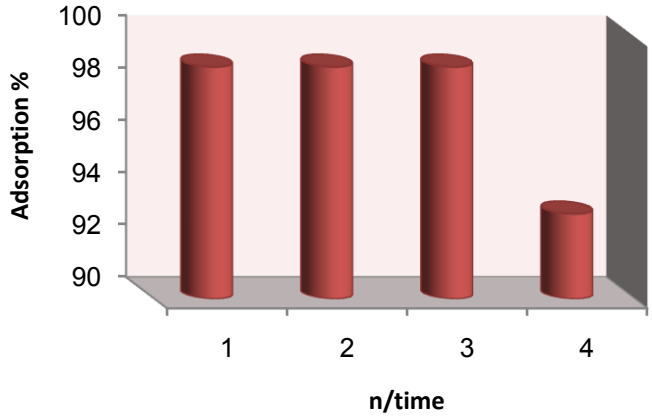

Figure 11: Effect of recycled NPs-MSK-Fe adsorbent on calmagite dye adsorption percent

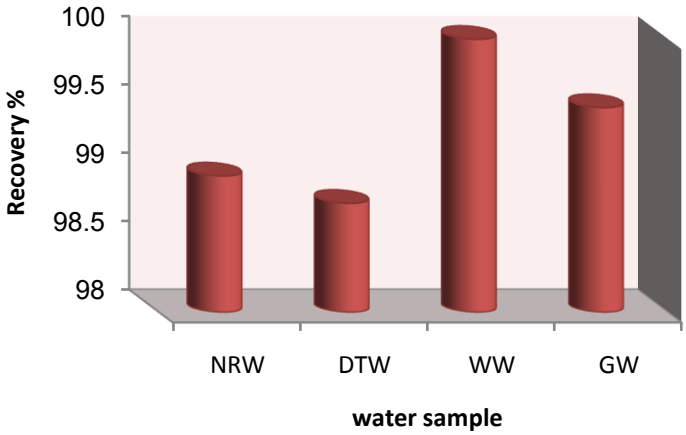

Figure 12: Recovery of calmagite dye spiked environmental water samples with NPs-MSK-Fe adsorbent at pH =2.0

4. Conclusion

The NPs-MSK-Fe adsorbent was prepared using simple procedure through impregnation process. The characteristics of both NPs-MSK and NPs-MSK-Fe adsorbents were identified by using FT-IR, TEM, SEM and X-ray techniques. The adsorption capacity of prepared NPs-MSK-Fe was investigated by batch experiments and equals 2125.7 µg g^{-1} which revealed that NPs-MSK-Fe adsorbent was effectively removing of calmagite dye. This new adsorbent can be regenerated by soaking in acidic ethanol solution of pH = 6.0 to recover both the adsorbents and the adsorbed dye. Also, the NPs-MSK-Fe adsorbent was applied for the removal of calmagite dye from environmental water samples with high recovery values and no matrix interference.

References

Adhoum, N., Monser, L. (2002): Removal of cyanide from aqueous solution using impregnated activated carbon. Chemical Engineering and Processing, 41: 17–21.

Ahmed, S.A. (2011): Batch and fixed-bed column techniques for removal of Cu(II) and Fe(III) usingcarbohydrate natural polymer modified complexing agents. Carbohydrate Polymers, 83: 1470–1478.

Bello, O.S., Olusegun, O.A., Njoku, V.O. (2013): Fly ash: an alternative to powdered activated carbon for the removal of eosin dye from aqueous solutions. Bull. Chem. Soc. Ethiop., 27: 191–204.

Bhatnagar, A.,Sillanpää, M. (2010): Utilization of agro-industrial and municipal waste materials as potential adsorbents for water treatment—A review. Chemical Engineering Journal, 157: 277–296.

Demirbas, E., Kobya, M., Sulak, M.T. (2008): Adsorption kinetics of a basic dye from aqueous solutions onto apricot stone activated carbon. Bioresource Technology, 99: 5368–5373.

Diaz, A., Coto, G. (1983): Chemical composition of two varieties of mango seed for animal feeding. Cuban Journal of Agricultural Science, 17: 175–182.

Dou, X., Zhang, Y., Wang, H., Wang, T., Wang, Y. (2011): Performance of granular zirconium–iron oxide in the removal of fluoride from drinking water. Water Res., 45: 3571–3578.

Elizalde-Gonzàlez, M.P., Hernàndez-Montoya, V. (2007): Characterization of mango pit as raw material in the preparation of activated carbon for wastewater treatment. Biochemical Engineering Journal, 36: 230–238.

Fazary, A.E., Taha, M., Ju, Y. (2009): Iron Complexation Studies of Gallic Acid, J. Chem. Eng. Data, 54: 35–42.

Ghanizadeh, Gh.,Ehrampoush, M.H., Ghaneian, M.T. (2010): Application of iron impregnated activated carbon for removal of arsenic from water. Iran. J. Environ. Health. Sci. Eng., 7: 145–156.

Gupta, V.K., Suhas. (2009): Application of low-cost adsorbents for dye removal – A review. Journal of Environmental Management, 90: 2313–2342.

Hamdaoui, O. (2006): Batch study of liquid-phase adsorption of methylene blue using cedar sawdust and crushed brick. J. Hazard. Mater., 135: 264–273.

Kanawade, S.M., Gaikwad, R.W., Misal, S.A. (2010): Low cost Sugarcane Bagasse Ash as an adsorbent for Dye Removal from Dye Effluent. International Journal of Chemical Engineering and Applications, 1: 309–318.

Kroschwitz, J.I., Howe-Grant, M. (1993): Kirk-Othmer Encyclopedia of Chemical Technology, fourth ed., Wiley, New York, pp 516–541.

Kumara, K.V., Kumaranb, A. (2005): Removal of methylene blue by mango seed kernel powder. Biochemical Engineering Journal, 27: 83–93.

Luo, X., Zhan, Y., Tu, X., Huang, Y., Luo, S., Yan, L. (2011): Novel molecularly imprinted polymer using 1-(α-methyl acrylate)-3-methylimidazolium bromide as functional monomer for simultaneous extraction and determination of water-soluble acid dyes in wastewater and soft drink by solid phase extraction and high performance liquid chromatography. Journal of Chromatography A, 1218: 1115–1121.

Madrakian, T., Afkhami, A., Ahmadi, M. (2012): Adsorption and kinetic studies of seven different organic dyes onto magnetite nanoparticles loaded tea waste and removal of them from wastewater samples. SpectrochimicaActa Part A: Molecular and Biomolecular Spectroscopy, 99: 102–109.

Namasivayam, C., Sangeetha, D. (2006): Recycling of agricultural solid waste, coirpith: removal of anions, heavy metals, organics and dyes from water by adsorption onto $ZnCl_2$ activated coirpith carbon. J. Hazard. Mater. B, 135: 449–452.

Panayiot, P.E., Stjamesb, B.St.J. (2009): Submicron structures from organometallic precursors, Faculty of the WORCESTER POLYTECHNIC INSTITUTE.

Panneerselvam, P., Morad, N., Tan, K.A. (2011): Magnetic nanoparticle (Fe_3O_4) impregnated onto tea waste for the removal of nickel(II) from aqueous solution. J. Hazard. Mater., 186: 160–168.

Pinheiro, H.M., Touraud, E., Thomas, O. (2004): Aromatic amines from azo dye reduction: status review with emphasis on direct UV spectrophotometric detection in textile industry wastewaters. Dyes Pigments, 61: 121–139.

Reddy, D.H.K., Lee, S. (2013): Application of magnetic chitosan composites for the removal of toxic metal and dyes from aqueous solutions. Advances in Colloid and Interface Science, 201–202: 68–93.

Reddy, M.P., Venugopal, A., Subrahmanyam, M. (2007): Hydroxyapatite photocatalytic degradation of calmagite (an azo dye) in aqueous suspension. Applied Catalysis B: Environmental, 69: 164–170.

Salem, N.M., Farhan, A.M., Awwad, A.M. (2012): Biosorption of Cadmium (II) from Aqueous Solutions by PrunusAvium Leaves. American Journal of Environmental Engineering, 2: 123–127.

Sandhu, K.S., Lim, S. (2008). Structural characteristics and in vitro digestibility of Mango kernel starches (Mangiferaindica L.). Food Chemistry, 107: 92–97.

Sharma, P.,Kaur, R., Baskar, C., Chung, W. (2010): Removal of methylene blue from aqueous waste using rice husk and rice husk ash. Desalination, 259: 249–257.

Sharma, Y.C., Srivastava, V., Weng, C.H., Upadhyay, S.N. (2009): Removal of Cr (VI) from Wastewater by Adsorption on Iron Nanoparticles. Can. J. Chem. Eng., 87: 921–929.

Sheibani, A., Shishehbor, M.R., Alaei, H. (2012): Removal of Fe(III) ions from aqueous solution by hazelnut hull as an adsorbent, International Journal of Industrial Chemistry, 3-4:1–4.

Singh, D.K., Srivastava, B. (1999): Removal of basic dyes from aqueous solutions by chemically treated Psidiumguyava leaves. Indian J. Environ. Health, 41: 333–345.

Soliman, E.M., Albishri, H.M., Marwani, H.M., Batterjee, M.G. (2013): Removal of 2-chlorophenol from aqueous solutions using activated carbon-impregnated Fe(III). Desalination and Water Treatment, 51: 1–8.

Soong, Y.Y., Barlow, P.J., 2006. Quantification of gallic acid and ellagic acid from longan (DimocarpuslonganLour.) seed and mango (Mangiferaindica L.) kernel and their effects on antioxidant activity. Food Chemistry 97, 524–530.

Soylak, M., Divrikli, U., Elci, L., Dogan, M., 2002.Preconcentration of Cr(III), Co(II), Cu(II), Fe(III) and Pb(II) as calmagite chelates on cellulose nitrate membrane filter prior to their flame atomic absorption spectrometric determinations. Talanta 56, 565–570.

Yagub, M.T., Sen, T.K., Afroze, S., Ang, H.M., 2014. Dye and its removal from aqueous solution by adsorption–A review. Advances in Colloid and Interface Science 209, 172–184.

Yu, J.X., Li, B.H., Sun, X.M., Yuan, J., Chi, R.A., 2009. Polymer modified biomass of baker's yeast for enhancement adsorption of methylene blue, rhodamine B and basic magenta. J. Hazard. Mater. 168, 1147–1154.